

Fundamental limits in Bayesian thermometry and attainability via adaptive strategies

Mohammad Mehboudi,^{1,*} Mathias R. Jørgensen,^{2,†} Stella Seah,¹
Jonatan B. Brask,² Jan Kołodzyński,³ and Martí Perarnau-Llobet^{1,‡}

¹*Département de Physique Appliquée, Université de Genève, 1211 Geneva, Switzerland*

²*Department of Physics, Technical University of Denmark, 2800 Kongens Lyngby, Denmark*

³*Centre for Quantum Optical Technologies, Centre of New Technologies, University of Warsaw, 02-097 Warsaw, Poland*

We investigate the limits of thermometry using quantum probes at thermal equilibrium within the Bayesian approach. We consider the possibility of engineering interactions between the probes in order to enhance their sensitivity, as well as feedback during the measurement process, i.e., adaptive protocols. On the one hand, we obtain an ultimate bound on thermometry precision in the Bayesian setting, valid for arbitrary interactions and measurement schemes, which lower bounds the error with a quadratic (Heisenberg-like) scaling with the number of probes. We develop a simple adaptive strategy that can saturate this limit. On the other hand, we derive a no-go theorem for non-adaptive protocols that does not allow for better than linear (shot-noise-like) scaling even if one has unlimited control over the probes, namely access to arbitrary many-body interactions.

Introduction.—Preparing quantum systems at low temperatures is an essential task for development of quantum technologies [1–3]. Measuring temperature precisely is necessary to validate cooling and ensure the performance of quantum protocols, and has been demonstrated in cutting-edge experiments [4–12]; it is however challenging. Due to the scarcity of thermal fluctuations at such low temperatures, the relative error on thermometry can be enormous. Moreover, the fragility of quantum systems requires additional forward planning to minimise disturbance while maximising the information obtained. The theory of quantum thermometry is built to address these pivotal challenges [13, 14].

Quantum thermometry finds fundamental limits on precision [15–18] and designs protocols to achieve them in different platforms [19–22], and improve them thanks to quantum correlations [23, 24], coherence [25, 26], many-body interactions and criticality [27–32] or other resources [33, 34]. To date, such enhancements have been developed in the context of local thermometry, aiming at designing a thermometer that detects the smallest temperature variations around a known temperature [13, 14]. In many practical situations, however, one might not know the temperature accurately beforehand. Rather, one has limited prior knowledge about the temperature of the sample. Under such circumstances, Bayesian estimation is a more suitable approach, and has been the subject of a few recent studies [35–37].

The goal of this work is to set the ultimate bounds of Bayesian equilibrium thermometry, and to develop adaptive strategies to saturate them. It is insightful to first recall analogous results in the local approach to equilibrium thermometry [13, 14]. Within such a framework—contrary to dynamical approaches where the probe evolves according to some predefined model

parametrised by the temperature [38, 39], e.g. a superconducting qubit in radiometry [40]—the probe always thermalises to the temperature of the sample whose value is known *a priori*. In that case, for any unbiased estimator $\tilde{\theta}$ of the temperature θ_0 , the mean square error is inversely proportional to the heat capacity of the probe: $\Delta\tilde{\theta} \propto 1/C$ [15, 16, 29, 41]. For n -body probes, C can scale super-extensively with n in the vicinity of a critical point, with the ultimate bound $C \approx n^2/4$ [15, 42]—a quadratic scaling with the number of resources reminiscent of the Heisenberg scaling in quantum metrology [43]. Here, we show that similar bounds hold in the Bayesian approach, but adaptive strategies are needed to saturate them, contrary to the local case. In fact, we prove that any non-adaptive strategy necessarily leads to $\Delta\tilde{\theta} \propto 1/n$ for sufficiently large n —i.e., a shot-noise-like scaling [43]—a no-go result that holds even when arbitrary control over the n -body probe Hamiltonian is allowed. Thus, adaptive measurement strategies are a crucial ingredient for optimal thermometry whenever the temperature value is *a priori* not perfectly known.

Preliminaries and setup.— We consider estimation of the temperature θ_0 of a (possibly macroscopic) sample given some prior distribution $p(\theta)$ reflecting our initial knowledge on θ_0 . We assume we have at our disposal N copies of a d -dimensional system that we use as probes, which are much smaller than the sample. When put in contact with the sample, we assume that the probes eventually reach thermal equilibrium at temperature θ_0 . By measuring them we infer θ_0 . This corresponds to the framework of equilibrium thermometry, which is by nature robust [13, 14]. In order to establish fundamental bounds, we assume full control on the Hamiltonian of the probes, and in particular the ability to make them interact. Therefore, alternatively one can think of a d^N -dimensional probe, which constitutes our resource.

The thermometry process is divided into m rounds, each involving $n = N/m$ probes. Every round consists of: (I) preparation of the n -body probe, (II) interaction with the sample and thermalisation, (III) mea-

* mohammad.mehboudi@unige.ch

† matrj@fysik.dtu.dk

‡ marti.perarnaullobet@unige.ch

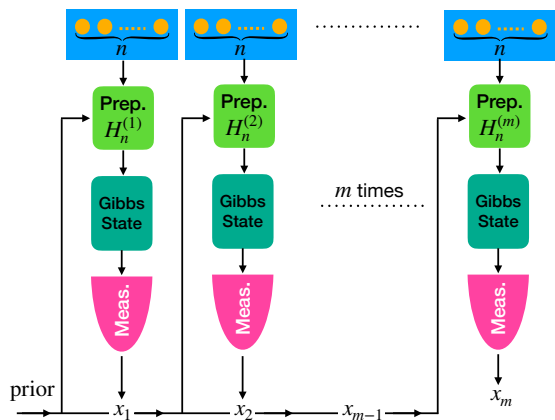


FIG. 1. Schematic representation of the adaptive scenario. A total of N probes are used in groups of n to estimate the temperature of the sample, θ_0 . Initially, our prior temperature distribution is given by $p(\theta)$, according to which we choose the Hamiltonian of the first n probes to be $H_n^{(1)}$ that minimises the expected mean square logarithmic error. The probes interact and thermalise with the sample followed by an energy measurement, yielding an outcome, say x_1 . Our knowledge about the temperature will be reflected in the posterior distribution $p(\theta|x_1)$. This will be used as the prior for the second round—in order to find the optimal Hamiltonian $H_n^{(2)}$. This process is repeated $m = N/n$ times. In contrast, in the non-adaptive scenario the Hamiltonian is fixed $H_n^{(k)} = H_n \forall k$.

surement/data acquisition, and (IV) data analysis (see Fig. 1). In the first round, we start by engineering the Hamiltonian $H_n^{(1)}$ of the n -body probe into any desired configuration based on the prior distribution $p(\theta)$. That is, we arrange the energy distribution of the n -body probe to become most sensitive to the relevant temperature range. Next, in step (II), this n -body system is put in contact with the sample, and reaches thermal equilibrium with it. Therefore, it can be described by the Gibbs state $\omega_{\theta_0}(H_n^{(1)}) := \exp[-H_n^{(1)}/\theta_0]/Z$, with $Z = \text{Tr}(\exp[-H_n^{(1)}/\theta_0])$ the partition function. Then, in step (III), a measurement is performed that yields an outcome x_1 . We focus on energy measurements since they are optimal as the Gibbs state is diagonal in the energy basis. In the data analysis (step (IV)), the posterior distribution is obtained through Bayes' rule:

$$p(\theta|x_1) = \frac{p(x_1|\theta)p(\theta)}{p(x_1)}, \quad (1)$$

where $p(x|\theta)$ is the likelihood function (which depends on the temperature *and* the Hamiltonian), $p(\theta)$ is the prior distribution on θ , and $p(x) = \int d\theta p(\theta)p(x|\theta)$ is the outcome probability. The next round proceeds in an analogous way, but replacing the prior $p(\theta)$ by $p(\theta|x_1)$ and $H_n^{(1)}$ by $H_n^{(2)}$. Likewise, in round $k > 1$, $p(\theta)$ is replaced by $p(\theta|\mathbf{x}_{k-1})$ with $\mathbf{x}_{k-1} \equiv \{x_{k-1}, \dots, x_2, x_1\}$ and $H_n^{(1)}$ is replaced by $H_n^{(k)}$. Such a strategy is adaptive since $H_n^{(k)}$

depends on \mathbf{x}_{k-1} . In contrast, a non-adaptive strategy satisfies $H_n^{(k)} = H_n \forall k$, where H_n is chosen according to the initial prior $p(\theta)$ only. At the end of the thermometry process (round m), the final estimate $\tilde{\theta}(\mathbf{x}_m)$ of θ_0 is computed.

In order to gauge the quality of the estimator, we need to introduce an error quantifier that describes how far θ is from θ_0 , on average. A natural measure which is suitable for equilibrium probes is the expected mean square logarithmic error (EMSLE) (see [35] for justification and the accompanying paper [44] for a deeper analysis and generalisation)

$$\text{EMSLE} := \int d\theta p(\theta) \int d\mathbf{x}_m p(\mathbf{x}_m|\theta) \ln^2 \left[\frac{\tilde{\theta}(\mathbf{x}_m)}{\theta} \right], \quad (2)$$

with $d\mathbf{x}_m := dx_m \dots dx_1$. Moreover,

$$\tilde{\theta}(\mathbf{x}_m) = \exp \left[\int d\theta \frac{p(\theta)p(\mathbf{x}_m|\theta)}{p(\mathbf{x}_m)} \ln \theta \right], \quad (3)$$

is the optimal temperature estimator, i.e., it minimises EMSLE [35].

We wish to find lower bounds for EMSLE, as well as optimal strategies to saturate them, for both adaptive and non-adaptive measurements. More precisely, our aim is to minimise EMSLE as a function of the number N of probes, with $N = mn$. We will pay particular attention to the relevant case where $m \gg 1$ is large (asymptotic regime) but n is limited due to e.g. experimental limitations on the amount of probes that can be collectively processed. In this case, we will focus on the scaling of EMSLE with n for a fixed but large m .

Main results.—Our main results are (i) an ultimate precision limit for Bayesian thermometry that holds for both adaptive and non-adaptive strategies, which in principle allows for a quadratic (Heisenberg-like) scaling with n , (ii) a no-go theorem that forbids super-extensive scaling in any non-adaptive scenario, and (iii) an adaptive strategy that reaches the ultimate limit. These results are derived in what follows (some technical details are given in the Appendix).

Given the prior $p(\theta)$, and by utilising the Van Trees inequality [45, 46] we construct a lower bound on the estimation error after m rounds

$$\text{EMSLE}^{-1} \leq Q[p(\theta)] + \sum_{k=1}^m \int d\mathbf{x}_{k-1} p(\mathbf{x}_{k-1}) \int d\theta p(\theta|\mathbf{x}_{k-1}) C(\theta; H_n^{(k)}), \quad (4)$$

where $p(\theta|\mathbf{x}_0) = p(\theta)$, $p(\mathbf{x}_0) = p(\mathbf{x}_0|\theta) = 1$, and $\int d\mathbf{x}_0 = 1$ are introduced to compress our notation. Here, $Q[p(\theta)]$ quantifies the prior information and reads

$$Q[p(\theta)] := \int d\theta p(\theta) [1 + \theta \partial_\theta \log p(\theta)]^2. \quad (5)$$

The second term quantifies the information acquired through all measurements. It also establishes a connection to the quantum Fisher information through its

proportionality to the heat capacity [15]. The heat capacity of the probe at round k of the measurement is denoted $C(\theta; H_n^{(k)})$, with the Hamiltonian $H_n^{(k)}$ designed according to the prior *and* the information acquired so far. Recall that, by definition, $C(\theta; H_n) := \partial_\theta E(\theta; H_n)$ where $E(\theta; H) = \text{Tr}[H\omega_\theta(H)]$ is the energy of the probe at thermal equilibrium. To bound Eq. (4), we first define the maximum of the integrand over $\{H_n^{(k)}\}_{k=1}^m$ for a specific trajectory \mathbf{x}_m :

$$\begin{aligned} \Gamma(\mathbf{x}_m) &:= \max_{\{H_n^{(k)}\}_k} \sum_{k=1}^m \int d\theta p(\theta|\mathbf{x}_{k-1}) C(\theta; H_n^{(k)}) \\ &\leq \sum_{k=1}^m \int d\theta p(\theta|\mathbf{x}_{k-1}) C_D = mC_D \end{aligned} \quad (6)$$

where $C_D := \max_{H_n} C(\theta; H_n)$, i.e., the maximum heat capacity of an n -body probe. In the last line we used that C_D is independent of θ (see [15] and the Appendix for the explicit expression of C_D). Furthermore, we have $C_D \approx \frac{n^2}{4} \log^2 d$, for large enough n . Putting everything together, we obtain from (4):

$$\begin{aligned} \text{EMSLE}^{-1} &\leq Q[p(\theta)] + mC_D \\ &\stackrel{n \gg 1}{\approx} Q[p(\theta)] + m \frac{n^2}{4} \log^2 d. \end{aligned} \quad (7)$$

This gives an ultimate bound on Bayesian thermometry [Result (i)], which both adaptive and non-adaptive strategies should respect. This bound implies that any Bayesian thermometry protocol is ultimately limited by a quadratic Heisenberg-like scaling.

The ultimate bound (7) becomes tight and can be saturated by adaptive strategies in the regime $m \gg 1$ (see results below). However, non-adaptive strategies fail to saturate it, and in fact EMSLE^{-1} can increase at most linearly with n [Result (ii)]

$$\text{EMSLE}^{-1} \stackrel{\text{non-adaptive}}{\leq} Q[p(\theta)] + f[p(\theta)]mn \log d, \quad (8)$$

where $f[p(\theta)] = \int_{\mathcal{R}} d\theta [-\partial_\theta p(\theta)]\theta$ is a functional of only the prior distribution, and \mathcal{R} is the temperature domain where $\partial_\theta p(\theta) \leq 0$. This result is rigorously proven in the Appendix, but let us provide some intuition. It is already noted in the literature that engineered probes for thermometry show enhanced sensitivity only in a small temperature range Δ [13, 15, 47–49]. Finite-size scaling theory hints that if $C \propto n^{1+\alpha}$, then $\Delta \propto n^{-\gamma}$ with $\gamma \geq \alpha$ in order to ensure that the energy density of an equilibrium state remains finite [50]. This implies that, for any $p(\theta)$ with a finite width (independent of n), the term $\int d\theta p(\theta)C(\theta)$ in Eq. (4) grows at most linearly with n for sufficiently large n . In other words, optimal n -body probes require priors with a width smaller than $\mathcal{O}(1/n)$ to obtain super-linear scaling, and conversely a finite width in $p(\theta)$ will eventually kill any super-linear scaling. The no-go result (B26) makes this intuition rigorous.

The above reasoning also explains why adaptive protocols can potentially saturate (7). By updating the prior $p(\theta)$ to the posterior $p(\theta|\mathbf{x}_{k-1})$ in each step of the process ($k = 1, \dots, m$), it can stay inside the optimal region for sufficiently large m , thus enabling super-linear precision. This also suggests using optimal probes for local thermometry as an *ansatz* for the Bayesian thermometry with adaptive strategies. The optimal thermometer in the local scenario is an effective two-level system with $d^n - 1$ -fold degeneracy in the excited state [15]. Although this Hamiltonian is useful to obtain fundamental bounds [15] it involves n -body interactions and is hence highly complex for $n \gg 1$. Nonetheless, it can be well approximated through two-body interactions by the method developed in [51] and, furthermore, it can be effectively realised with a few-fermionic mixture confined in a one-dimensional harmonic trap [42]. Motivated by this progress, at the k th round we restrict to the class of Hamiltonians $H_n^{(k)}$ with the aforementioned two-level structure, and tune the energy gap to minimise the EMSLE (2). As we show in the example below, we can achieve a quadratic scaling with n and saturate (7) using this strategy [Result (iii)].

Case study.—The results presented here are valid for a broad class of priors, but in what follows we stick to a specific choice in order to illustrate their usage. In any relevant application of thermometry, the temperature is known a priori to lie within a certain range, i.e., $\theta_{\min} \leq \theta_0 \leq \theta_{\max}$. We use a family of probability distributions that are suitable in this case and were proposed in [52]:

$$p(\theta) = \frac{1}{k_\alpha(\theta_{\max} - \theta_{\min})} \left[e^{\alpha \sin^2\left(\pi \frac{\theta - \theta_{\min}}{\theta_{\max} - \theta_{\min}}\right)} - 1 \right] \quad (9)$$

with

$$k_\alpha := e^{\alpha/2} I_0(\alpha/2) - 1, \quad (10)$$

where I_0 is the modified Bessel function of the first kind. In the limit $\alpha \rightarrow -\infty$ the above prior becomes a constant, while in the limit $\alpha \rightarrow 0$ we have $p(\theta) \propto \sin^2(2\theta)$.

The adaptive strategy works as follows. We consider as a resource N qubits, which are divided in m groups of n qubits. In each group, the n -qubit Hamiltonian is engineered to become a two-level system with degeneracy $(2^n - 1)$ and with a tunable gap ϵ . In the first round, we tune the gap to $\epsilon^{(1)}$ to minimise the single shot EMSLE, that is we set $m = 1$ in (2). Then, we measure the energy of the system. Given the outcome x_1 is observed, we update the prior to $p(\theta) \rightarrow p(\theta|x_1)$, and implement the same procedure to choose $\epsilon^{(2)}$ in the second round (i.e., we minimise (2) replacing $p(\theta) \rightarrow p(\theta|x_1)$). This process is repeated until all probes are used.

In our simulations, we apply the adaptive process for a given θ_0 sampled from $p(\theta)$, which yields a trajectory as illustrated in the left panel of Fig. 2. We see that the prior peaks around the true temperature as k increases, and the estimated temperature gets closer to the true temperature, i.e., $\hat{\theta}/\theta_0 \rightarrow 1$. The average over a large amount of

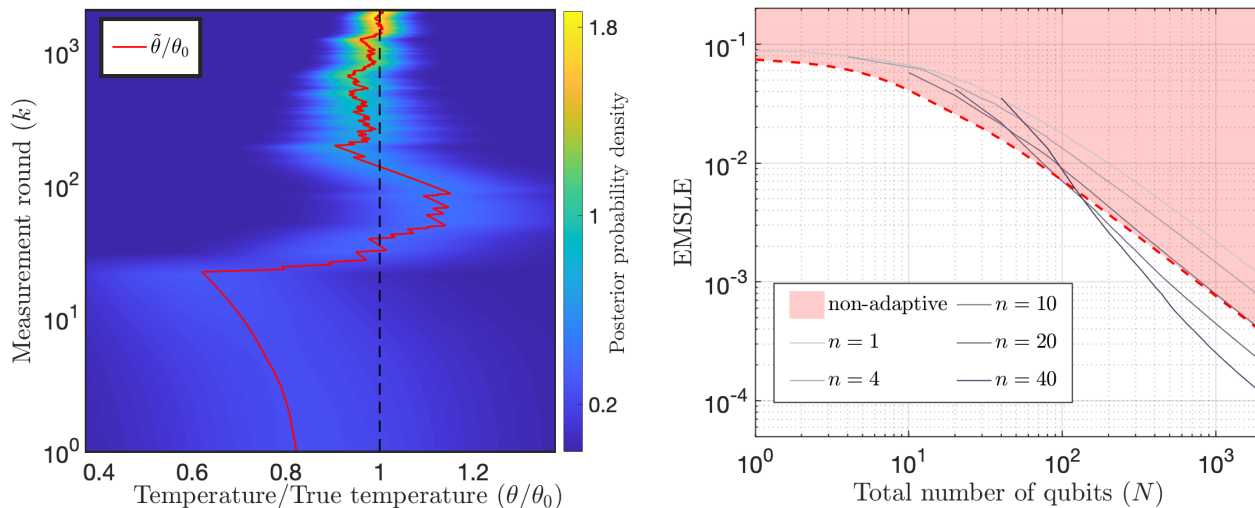


FIG. 2. Left—Contour plot of the prior versus the measurement round $k \in \{1, \dots, m\}$ (logarithmic scale), and temperature normalised to its true value θ/θ_0 . The red trajectory shows the ratio between the estimated temperature and the true temperature $\tilde{\theta}/\theta_0$. As k increases, the prior sharpens around the true temperature, and $\tilde{\theta}/\theta_0$ approaches one. Here, we have set $n = 1$, $\alpha = 1$, $\theta_{\min} = 1$, and $\theta_{\max} = 10$ in arbitrary units. Right—Loglog plot of the expected mean square logarithmic error (EMSLE) attained by the adaptive strategy vs. the total number of qubits N . Dark solid lines represent different values of n . They show that, for sufficiently large N , the bigger n is the smaller the error can get. The red-dashed line is the (not necessarily tight) bound on non-adaptive strategies: only the shaded area can be achieved using non-adaptive protocols. One can cross the border with adaptive strategies for $n > 10$.

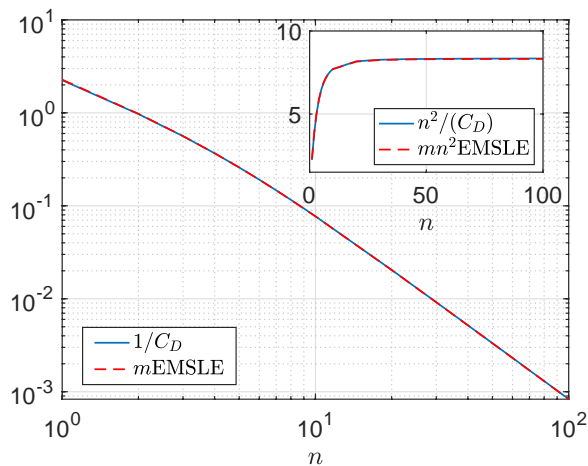


FIG. 3. (Dashed red) Loglog plot of the normalised expected mean square logarithmic error (EMSLE) after m rounds of the adaptive scheme—for sufficiently large m , here $m = 2 \times 10^3$ —vs n . This shows that for large enough n the error vanishes quadratically with n , which can be better seen from the inset. (Blue) The minimum achievable EMSLE given by the r.h.s of (7). The perfect agreement shows the efficiency of the proposed adaptive protocol.

trajectories enables us to compute EMSLE in Eq. (2) with high accuracy (in the numerical simulations, we consider $\mathcal{O}(1000/m)$ trajectories, which ensures convergence). In the right panel of Fig. 3 we plot EMSLE in the adaptive

scenario for various values of n , benchmarked against the no-go bound for non-adaptive scenarios—only the shaded area can be accessed by non-adaptive strategies given any $n \leq N$. We see that as n increases the error gets smaller for large enough N . In particular, there exist some threshold n for which one can beat the no-go bound via adaptive strategies. As an example, given $N = 10^3$ and $\theta_{\max}/\theta_{\min} = 10$ in Eq. (9) (with $\alpha = 1$), adaptive strategies using $n \approx 10$ interacting qubits outperform arbitrary non-adaptive strategies.

Next, we ask whether the adaptive strategy can reach the Heisenberg-like scaling, $\text{EMSLE}^{-1} \propto mn^2$. To this aim, we study the behaviour of the error with the resources n for a sufficiently large number of repetitions m . The results are depicted in Fig. 3, where we see Eq. (7) is saturated and therefore the proposed adaptive scheme reaches the ultimate bound on thermometry.

Finally, we note that although the optimal protocol requires a very idealised Hamiltonian for the probe (a $(2^n - 1)$ -degenerate two-level system), adaptive protocols already become useful for small n . Namely for $n = 1, 2$, they decrease the error more than 60% and 80%, respectively compared to the non-adaptive protocols (see SM for details). For larger n , a realistic method to obtain a scaling of the EMSLE beyond the SNL would be to combine the adaptive method derived here with thermal phase transitions [50].

Conclusions and future directions.—We derived fundamental limitations of the Bayesian approach to equilibrium thermometry, which shows a Heisenberg-like

quadratic scaling with the number of probes. We showed non-adaptive strategies cannot saturate this bound and, are limited to shot-noise-like scaling whenever the initial prior is not sharp. We also constructed an adaptive protocol that saturates the ultimate bound, thus highlighting the crucial role of adaptivity in quantum thermometry. This is importantly different to Bayesian phase-estimation protocols [53], where the Heisenberg limit that applies to most general adaptive protocols [54] can be attained by resorting only to measurements being adaptively varied in between the phase-encoding channel uses [55]. In contrast, in equilibrium thermometry the form of probe states (Gibbs) and measurement (energy-basis) is fixed, and it is the probe Hamiltonian that must be adaptively adjusted for the quadratic scaling to become reachable.

While here we considered the total number of probes N as our resource, future works could include time as an extra resource. This naturally leads to non-equilibrium thermometry, where the probe is measured before reach-

ing thermalisation. While considerable progress in this framework has been obtained within the frequentist approach [13, 25, 38, 39, 56, 57], adaptive protocols could be developed following the Bayesian approach pursued here. Lastly, exploiting adaptive schemes for other metrological tasks involving criticality and quantum phase transitions [58], or restrictions such as limited measurement resolution [17, 18, 59], can be subject of future work.

Acknowledgements.—We gratefully thank J. Rubio and L. A. Correa for fruitful discussions in an early stage of this work. M.M. and M.P.-L. acknowledge financial support from the Swiss National Science Foundation (NCCR SwissMAP and Ambizione grant PZ00P2-186067). J.K. acknowledges the Foundation for Polish Science within the “Quantum Optical Technologies” project carried out within the International Research Agendas programme cofinanced by the European Union under the European Regional Development Fund. MRJ and JBB acknowledge support by the Independent Research Fund Denmark.

-
- [1] Alessio Celi, Anna Sanpera, Veronica Ahufinger, and Maciej Lewenstein, “Quantum optics and frontiers of physics: the third quantum revolution,” *Physica Scripta* **92**, 013003 (2016).
- [2] Immanuel Bloch, Jean Dalibard, and Wilhelm Zwerger, “Many-body physics with ultracold gases,” *Rev. Mod. Phys.* **80**, 885–964 (2008).
- [3] Immanuel Bloch, Jean Dalibard, and Sylvain Nascimbene, “Quantum simulations with ultracold quantum gases,” *Nature Physics* **8**, 267–276 (2012).
- [4] AE Leanhardt, TA Pasquini, Michele Saba, A Schirotzek, Y Shin, David Kielpinski, DE Pritchard, and W Ketterle, “Cooling bose-einstein condensates below 500 picokelvin,” *Science* **301**, 1513–1515 (2003).
- [5] Quentin Bouton, Jens Nettersheim, Daniel Adam, Felix Schmidt, Daniel Mayer, Tobias Lausch, Eberhard Tiesmann, and Artur Widera, “Single-atom quantum probes for ultracold gases boosted by nonequilibrium spin dynamics,” *Phys. Rev. X* **10**, 011018 (2020).
- [6] Marco Scigliuzzo, Andreas Bengtsson, Jean-Claude Besse, Andreas Wallraff, Per Delsing, and Simone Gasparinetti, “Primary thermometry of propagating microwaves in the quantum regime,” *Phys. Rev. X* **10**, 041054 (2020).
- [7] Ryan Olf, Fang Fang, G Edward Marti, Andrew MacRae, and Dan M Stamper-Kurn, “Thermometry and cooling of a bose gas to 0.02 times the condensation temperature,” *Nature Physics* **11**, 720–723 (2015).
- [8] Rudolf Gati, Børge Hemmerling, Jonas Fölling, Michael Albiez, and Markus K. Oberthaler, “Noise thermometry with two weakly coupled bose-einstein condensates,” *Phys. Rev. Lett.* **96**, 130404 (2006).
- [9] Alberto Ronzani, Bayan Karimi, Jordan Senior, Yu-Cheng Chang, Joonas T Peltonen, ChiiDong Chen, and Jukka P Pekola, “Tunable photonic heat transport in a quantum heat valve,” *Nature Physics* **14**, 991–995 (2018).
- [10] F. M. Spiegelhalter, A. Trenkwalder, D. Naik, G. Hendl, F. Schreck, and R. Grimm, “Collisional stability of ^{40}K immersed in a strongly interacting fermi gas of ^6Li ,” *Phys. Rev. Lett.* **103**, 223203 (2009).
- [11] Kuan Yen Tan, Matti Partanen, Russell E Lake, Joonas Govenius, Shumpei Masuda, and Mikko Möttönen, “Quantum-circuit refrigerator,” *Nature communications* **8**, 1–8 (2017).
- [12] Daniel Adam, Quentin Bouton, Jens Nettersheim, Sabrina Burgardt, and Artur Widera, “Coherent and dephasing spectroscopy for single-impurity probing of an ultracold bath,” [arXiv preprint arXiv:2105.03331](https://arxiv.org/abs/2105.03331) (2021).
- [13] Mohammad Mehboudi, Anna Sanpera, and Luis A Correa, “Thermometry in the quantum regime: recent theoretical progress,” *Journal of Physics A: Mathematical and Theoretical* **52**, 303001 (2019).
- [14] Antonella De Pasquale and Thomas M Stace, “Quantum thermometry,” in *Thermodynamics in the Quantum Regime* (Springer, 2018) pp. 503–527.
- [15] Luis A. Correa, Mohammad Mehboudi, Gerardo Adesso, and Anna Sanpera, “Individual quantum probes for optimal thermometry,” *Phys. Rev. Lett.* **114**, 220405 (2015).
- [16] Matteo G A Paris, “Achieving the landau bound to precision of quantum thermometry in systems with vanishing gap,” *Journal of Physics A: Mathematical and Theoretical* **49**, 03LT02 (2015).
- [17] Patrick P. Potts, Jonatan Bohr Brask, and Nicolas Brunner, “Fundamental limits on low-temperature quantum thermometry with finite resolution,” *Quantum* **3**, 161 (2019).
- [18] Mathias R. Jørgensen, Patrick P. Potts, Matteo G. A. Paris, and Jonatan B. Brask, “Tight bound on finite-resolution quantum thermometry at low temperatures,” *Phys. Rev. Research* **2**, 033394 (2020).
- [19] Mohammad Mehboudi, Aniello Lampo, Christos Charalambous, Luis A. Correa, Miguel Ángel García-March, and Maciej Lewenstein, “Using polarons for sub-nk quantum nondemolition thermometry in a bose-einstein con-

- densate,” *Phys. Rev. Lett.* **122**, 030403 (2019).
- [20] Gerardo A. Paz-Silva, Leigh M. Norris, and Lorenza Viola, “Multiqubit spectroscopy of gaussian quantum noise,” *Phys. Rev. A* **95**, 022121 (2017).
- [21] J. Ruostekoski, C. J. Foot, and A. B. Deb, “Light scattering for thermometry of fermionic atoms in an optical lattice,” *Phys. Rev. Lett.* **103**, 170404 (2009).
- [22] Mark T. Mitchison, Thomás Fogarty, Giacomo Guarnieri, Steve Campbell, Thomas Busch, and John Goold, “In situ thermometry of a cold fermi gas via dephasing impurities,” *Phys. Rev. Lett.* **125**, 080402 (2020).
- [23] Stella Seah, Stefan Nimmrichter, Daniel Grimmer, Jader P. Santos, Valerio Scarani, and Gabriel T. Landi, “Collisional quantum thermometry,” *Phys. Rev. Lett.* **123**, 180602 (2019).
- [24] Steve Campbell, Mohammad Mehboudi, Gabriele De Chiara, and Mauro Paternostro, “Global and local thermometry schemes in coupled quantum systems,” *New Journal of Physics* **19**, 103003 (2017).
- [25] Sania Jevtic, David Newman, Terry Rudolph, and T. M. Stace, “Single-qubit thermometry,” *Phys. Rev. A* **91**, 012331 (2015).
- [26] Sholeh Razavian, Claudia Benedetti, Matteo Bina, Yahya Akbari-Kourbolagh, and Matteo GA Paris, “Quantum thermometry by single-qubit dephasing,” *The European Physical Journal Plus* **134**, 284 (2019).
- [27] Antonella De Pasquale, Davide Rossini, Rosario Fazio, and Vittorio Giovannetti, “Local quantum thermal susceptibility,” *Nature communications* **7**, 1–8 (2016).
- [28] Karen V. Hovhannisyán and Luis A. Correa, “Measuring the temperature of cold many-body quantum systems,” *Phys. Rev. B* **98**, 045101 (2018).
- [29] M Mehboudi, M Moreno-Cardoner, G De Chiara, and A Sanpera, “Thermometry precision in strongly correlated ultracold lattice gases,” *New Journal of Physics* **17**, 055020 (2015).
- [30] Safoura S. Mirkhalaf, Daniel Benedicto Orenes, Morgan W. Mitchell, and Emilia Witkowska, “Criticality-enhanced quantum sensing in ferromagnetic bose-einstein condensates: Role of readout measurement and detection noise,” *Phys. Rev. A* **103**, 023317 (2021).
- [31] C L Latune, I Sinayskiy, and F Petruccione, “Collective heat capacity for quantum thermometry and quantum engine enhancements,” *New Journal of Physics* **22**, 083049 (2020).
- [32] Guim Planella, Marina F. B. Cenni, Antonio Acín, and Mohammad Mehboudi, “Bath-induced correlations enhance thermometry precision at low temperatures,” *Phys. Rev. Lett.* **128**, 040502 (2022).
- [33] Luis A. Correa, Martí Perarnau-Llobet, Karen V. Hovhannisyán, Sneider Hernández-Santana, Mohammad Mehboudi, and Anna Sanpera, “Enhancement of low-temperature thermometry by strong coupling,” *Phys. Rev. A* **96**, 062103 (2017).
- [34] Patrick P. Hofer, Jonatan Bohr Brask, Martí Perarnau-Llobet, and Nicolas Brunner, “Quantum thermal machine as a thermometer,” *Phys. Rev. Lett.* **119**, 090603 (2017).
- [35] Jesús Rubio, Janet Anders, and Luis A. Correa, “Global quantum thermometry,” *Phys. Rev. Lett.* **127**, 190402 (2021).
- [36] Gabriel O. Alves and Gabriel T. Landi, “Bayesian estimation for collisional thermometry,” *Phys. Rev. A* **105**, 012212 (2022).
- [37] Julia Boeyens, Stella Seah, and Stefan Nimmrichter, “Uninformed bayesian quantum thermometry,” *Phys. Rev. A* **104**, 052214 (2021).
- [38] Alexander Holm Kiilerich, Antonella De Pasquale, and Vittorio Giovannetti, “Dynamical approach to ancilla-assisted quantum thermometry,” *Phys. Rev. A* **98**, 042124 (2018).
- [39] Stella Seah, Stefan Nimmrichter, Daniel Grimmer, Jader P. Santos, Valerio Scarani, and Gabriel T. Landi, “Collisional quantum thermometry,” *Phys. Rev. Lett.* **123**, 180602 (2019).
- [40] Zhixin Wang, Mingrui Xu, Xu Han, Wei Fu, Shruti Puri, S. M. Girvin, Hong X. Tang, S. Shankar, and M. H. Devoret, “Quantum microwave radiometry with a superconducting qubit,” *Phys. Rev. Lett.* **126**, 180501 (2021).
- [41] T. Jahnke, S. Lanéry, and G. Mahler, “Operational approach to fluctuations of thermodynamic variables in finite quantum systems,” *Phys. Rev. E* **83**, 011109 (2011).
- [42] Marcin Płodzień, Rafał Demkowicz-Dobrzański, and Tomasz Sowiński, “Few-fermion thermometry,” *Phys. Rev. A* **97**, 063619 (2018).
- [43] Vittorio Giovannetti, Seth Lloyd, and Lorenzo Maccone, “Quantum-enhanced measurements: beating the standard quantum limit,” *Science* **306**, 1330–1336 (2004).
- [44] Mathias R. Jørgensen, Jan Kolodyński, Mohammad Mehboudi, Martí Perarnau-Llobet, and Jonatan B. Brask, “Bayesian quantum thermometry based on thermodynamic length,” *Phys. Rev. A* **105**, 042601 (2022).
- [45] Harry L Van Trees, *Detection, estimation, and modulation theory, part I: detection, estimation, and linear modulation theory* (John Wiley & Sons, 2004).
- [46] Harry L Van Trees and Kristine L Bell, *Bayesian bounds for parameter estimation and nonlinear filtering/tracking* (Wiley-IEEE press New York, 2007).
- [47] Steve Campbell, Marco G Genoni, and Sebastian Deffner, “Precision thermometry and the quantum speed limit,” *Quantum Science and Technology* **3**, 025002 (2018).
- [48] Ricardo Román-Ancheyta, Barış Çakmak, and Özgür E Müstecaplıođlu, “Spectral signatures of non-thermal baths in quantum thermalization,” *Quantum Science and Technology* **5**, 015003 (2019).
- [49] Wai-Keong Mok, Kishor Bharti, Leong-Chuan Kwek, and Abolfazl Bayat, “Optimal probes for global quantum thermometry,” arXiv preprint arXiv:2010.14200 (2020).
- [50] Kerson Huang, *Introduction to statistical physics* (Chapman and Hall/CRC, 2009).
- [51] Nicholas Chancellor, Stefan Zohren, Paul A Warburton, Simon C Benjamin, and Stephen Roberts, “A direct mapping of max k-sat and high order parity checks to a chimera graph,” *Scientific reports* **6**, 1–9 (2016).
- [52] Yan Li, Luca Pezzè, Manuel Gessner, Zhihong Ren, Weidong Li, and Augusto Smerzi, “Frequentist and bayesian quantum phase estimation,” *Entropy* **20** (2018), 10.3390/e20090628.
- [53] D. W. Berry and H. M. Wiseman, “Optimal states and almost optimal adaptive measurements for quantum interferometry,” *Phys. Rev. Lett.* **85**, 5098–5101 (2000).
- [54] Wojciech Górecki, Rafał Demkowicz-Dobrzański, Howard M. Wiseman, and Dominic W. Berry, “ π -corrected heisenberg limit,” *Phys. Rev. Lett.* **124**, 030501 (2020).

- [55] H. M. Wiseman, D. W. Berry, S. D. Bartlett, B. L. Higgins, and G. J. Pryde, “Adaptive Measurements in the Optical Quantum Information Laboratory,” *IEEE Journal of Selected Topics in Quantum Electronics* **15**, 1661–1672 (2009).
- [56] Vasco Cavina, Luca Mancino, Antonella De Pasquale, Ilaria Gianani, Marco Sbroscia, Robert I. Booth, Emanuele Roccia, Roberto Raimondi, Vittorio Giovannetti, and Marco Barbieri, “Bridging thermodynamics and metrology in nonequilibrium quantum thermometry,” *Phys. Rev. A* **98**, 050101 (2018).
- [57] Marek M. Rams, Piotr Sierant, Omyoti Dutta, Paweł Horodecki, and Jakub Zakrzewski, “At the limits of criticality-based quantum metrology: Apparent superheisenberg scaling revisited,” *Phys. Rev. X* **8**, 021022 (2018).
- [58] Irénée Frérot and Tommaso Roscilde, “Quantum critical metrology,” *Phys. Rev. Lett.* **121**, 020402 (2018).
- [59] Karen V. Hovhannisyanyan, Mathias R. Jørgensen, Gabriel T. Landi, Álvaro M. Alhambra, Jonatan B. Brask, and Martí Perarnau-Llobet, “Optimal quantum thermometry with coarse-grained measurements,” *PRX Quantum* **2**, 020322 (2021).
- [60] Michael Ronen *et al.*, In preparation (2022).

Appendix A: Derivation of the Van Trees inequality

a. Preliminaries

We consider a continuous Euclidean one-dimensional parameter space $\Lambda \subseteq \mathbb{R}$. For a Euclidean space, a suitable function measuring the distance between parameter values is the absolute difference, i.e.

$$\mathcal{D}(\tilde{\lambda}, \lambda) = |\tilde{\lambda} - \lambda| \text{ for } \tilde{\lambda}, \lambda \in \Lambda. \quad (\text{A1})$$

Within the Bayesian approach to parameter estimation we start from a prior probability density $p(\lambda)$ over the parameter space Λ . The prior probability is updated as measurement data is acquired. Given measurement data $\mathbf{x}_m = \{x_1, \dots, x_m\}$, Bayes’ theorem allows us to express the update at measurement step k as

$$p(\lambda|\mathbf{x}_k) = \frac{p(x_k|\lambda, \mathbf{x}_{k-1})p(\lambda|\mathbf{x}_{k-1})}{p(x_k|\mathbf{x}_{k-1})}, \quad (\text{A2})$$

where in order to compress the notation we let $p(x_1|\lambda, \mathbf{x}_0) = p(x_1|\lambda)$, $p(\lambda|\mathbf{x}_0) = p(\lambda)$, and $p(x_1|\mathbf{x}_0) = p(x_1)$. Here, $p(x_k|\lambda, \mathbf{x}_{k-1})$ is the likelihood function associated with the implemented measurement. Note that this might be conditional on past measurement outcomes. We have also defined the marginal density

$$p(x_k|\mathbf{x}_{k-1}) := \int d\lambda p(x_k|\lambda, \mathbf{x}_{k-1})p(\lambda|\mathbf{x}_{k-1}). \quad (\text{A3})$$

For later convenience we introduce the joint probability density $p(\lambda, \mathbf{x}_k) = p(x_k|\lambda, \mathbf{x}_{k-1})p(\lambda, \mathbf{x}_{k-1})$, where it is understood that $p(\lambda, \mathbf{x}_0) = p(\lambda)$, and therefore $p(\mathbf{x}_0) = 1$ and $p(\mathbf{x}_0|\lambda) = 1$. Applying equation (A2) iteratively, we can write the posterior distribution resulting from the full measurement trajectory as

$$p(\lambda|\mathbf{x}_m) = \frac{p(\mathbf{x}_m|\lambda)p(\lambda)}{p(\mathbf{x}_m)}, \quad (\text{A4})$$

where we have defined

$$p(\mathbf{x}_m|\lambda) = \prod_{k=1}^m p(x_k|\lambda, \mathbf{x}_{k-1}) \quad (\text{A5})$$

$$p(\mathbf{x}_m) = \prod_{k=1}^m p(x_k|\mathbf{x}_{k-1}). \quad (\text{A6})$$

b. Mean-square distance estimation

An estimation theory is a prescription for specifying a parameter estimate $\bar{\lambda}(\mathbf{x}_m)$, computed as a function of the data, and for providing a measure of the confidence in the computed estimate. Here we employ the framework of *mean-square distance* (MSD) estimation, in which the confidence in an estimate is gauged by the posterior MSD:

$$\begin{aligned} \text{MSD}(\mathbf{x}_m) &:= \int d\lambda p(\lambda|\mathbf{x}_m) \mathcal{D}(\bar{\lambda}(\mathbf{x}_m), \lambda)^2, \\ &= \int d\lambda p(\lambda|\mathbf{x}_m) |\bar{\lambda}(\mathbf{x}_m) - \lambda|^2, \end{aligned} \quad (\text{A7})$$

where the second equality follows as we are considering a Euclidean parameter space. Given a measure of the confidence in an estimate, it is natural to find the maximum confidence estimator. It can be shown, by minimizing Eq. (A7) with respect to $\bar{\lambda}(\mathbf{x}_m)$, that the choice of estimator which minimizes the posterior MSD is the posterior mean

$$\bar{\lambda}(\mathbf{x}_m) = \int d\lambda p(\lambda|\mathbf{x}_m)\lambda. \quad (\text{A8})$$

In what follows, we exclusively consider the posterior mean, i.e. the *minimal mean-square distance* (MMSD) estimator. Since the MSD is a stochastic quantity defined for a single measurement trajectory, it is common to consider the *expected mean-square distance* (EMSD):

$$\text{EMSD} := \int d\lambda d\mathbf{x}_m p(\lambda, \mathbf{x}_m) |\bar{\lambda}(\mathbf{x}_m) - \lambda|^2, \quad (\text{A9})$$

which is obtained by averaging the MSD over the marginal distribution $p(\mathbf{x}_m)$. As the name suggest, this quantity gives the MSD which would be obtained on average, if the true parameter value is sampled from the prior probability.

c. The Van-Trees inequality

We now give a derivation of a Bayesian Cramér-Rao bound on the EMSD, in particular we consider the *Van Trees inequality* [45]. To derive the Bayesian bound we first define the quantity

$$\begin{aligned} \mathcal{H} := \int d\lambda d\mathbf{x}_m \sqrt{p(\lambda, \mathbf{x}_m)} (\bar{\lambda}(\mathbf{x}_m) - \lambda) \\ \times \sqrt{p(\lambda, \mathbf{x}_m)} \partial_\lambda \log p(\lambda, \mathbf{x}_m), \end{aligned} \quad (\text{A10})$$

where differentiability of the posterior distribution is implicitly assumed. The above quantity is clearly defined to motivate an application of the Cauchy-Schwarz inequality. From a direct evaluation of the above integral we find

$$\begin{aligned} \mathcal{H} &= \int d\lambda d\mathbf{x}_m (\bar{\lambda}(\mathbf{x}_m) - \lambda) \partial_\lambda p(\lambda, \mathbf{x}_m) \\ &= 1 + \int d\mathbf{x}_m \{ [\bar{\lambda}(\mathbf{x}_m) - \lambda] p(\lambda, \mathbf{x}_m) \}_{\lambda \in \mathcal{B}(\Lambda)}, \end{aligned} \quad (\text{A11})$$

where $\mathcal{B}(\Lambda)$ denotes the boundaries of the parameter space Λ . In most cases of interest the boundary term vanish. Here we take the vanishing of the boundary term as a constraint on the class of models considered, i.e.

$$p(\lambda, \mathbf{x}_m) = 0 \quad \text{for } \lambda \in \mathcal{B}(\Lambda) \quad (\text{A12})$$

$$\lambda p(\lambda, \mathbf{x}_m) = 0 \quad \text{for } \lambda \in \mathcal{B}(\Lambda). \quad (\text{A13})$$

Given these boundary conditions it follows that $\mathcal{H} = 1$. If we return to the definition of \mathcal{H} , i.e. equation (A10), and apply the Cauchy-Schwarz inequality, then we obtain the Van Trees inequality:

$$\begin{aligned} \text{EMSD}^{-1} &\leq \int d\lambda d\mathbf{x}_m p(\lambda, \mathbf{x}_m) [\partial_\lambda \log p(\lambda, \mathbf{x}_m)]^2 \\ &= Q[p(\lambda)] + \int d\lambda d\mathbf{x}_m p(\lambda, \mathbf{x}_m) [\partial_\lambda \log p(\mathbf{x}_m|\lambda)]^2, \end{aligned} \quad (\text{A14})$$

where the second equality follows directly from the decomposition $p(\lambda, \mathbf{x}_m) = p(\mathbf{x}_m|\lambda)p(\lambda)$ of the joint probability distribution, and we have defined the so-called Bayesian information of the prior distribution (which quantifies the prior information about the parameter λ) as [45]:

$$Q[p(\lambda)] := \int d\lambda p(\lambda) [\partial_\lambda \log p(\lambda)]^2. \quad (\text{A15})$$

We can put the Van Trees inequality into the form employed in the main text by decomposing the likelihood function using equation (A5), and then rewriting the expression using Bayes theorem:

$$\begin{aligned}
\text{EMSD}^{-1} &\leq Q[p(\lambda)] + \int d\lambda d\mathbf{x}_m p(\lambda, \mathbf{x}_m) \sum_{k=1}^m [\partial_\lambda \log p(x_k|\lambda, \mathbf{x}_{k-1})]^2 \\
&= Q[p(\lambda)] + \sum_{k=1}^m \int d\lambda d\mathbf{x}_{k-1} p(\lambda, \mathbf{x}_{k-1}) \int dx_k p(x_k|\lambda, \mathbf{x}_{k-1}) [\partial_\lambda \log p(x_k|\lambda, \mathbf{x}_{k-1})]^2 \\
&= Q[p(\lambda)] + \sum_{k=1}^m \int d\mathbf{x}_{k-1} p(\mathbf{x}_{k-1}) \int d\lambda p(\lambda|\mathbf{x}_{k-1}) h_k(\lambda)
\end{aligned} \tag{A16}$$

where

$$h_k(\lambda) := \int dx_k p(x_k|\lambda, \mathbf{x}_{k-1}) [\partial_\lambda \log p(x_k|\lambda, \mathbf{x}_{k-1})]^2. \tag{A17}$$

is just the Fisher Information of the distribution $p(x_k|\lambda, \mathbf{x}_{k-1})$ evaluated with respect to the parameter λ [45]. Note that the Fisher information $h_k(\lambda)$ is generally conditioned on the past measurement trajectory \mathbf{x}_{k-1} —a fact that we suppress in the notation for simplicity.

Appendix B: Application to equilibrium thermometry

a. Preliminaries

We now turn our attention to equilibrium probe thermometry. Let $\theta \in \Theta$ denote the sample temperature, where Θ is the space of temperatures. We consider a measurement consisting of first thermalizing the n -qudit probe system, described by a Hamiltonian operator $H_n^{(k)}$, and then performing a projective energy measurement of the probe. The probe at measurement step k is found in the thermal Gibbs state

$$\omega(\theta; H_n^{(k)}) = \frac{e^{-H_n^{(k)}/k_B\theta}}{\mathcal{Z}_n^{(k)}} \tag{B1}$$

with $\mathcal{Z}_n^{(k)} = \text{Tr}(e^{-H_n^{(k)}/k_B\theta})$, and k_B is Boltzmann's constant. For convenience, the ground-state energy is set to zero. The definitions of the average probe energy and the probe heat capacity are:

$$E(\theta; H_n^{(k)}) := \text{Tr}(H_n^{(k)}\omega(\theta; H_n^{(k)})), \tag{B2}$$

$$C(\theta; H_n^{(k)}) := \frac{dE(\theta; H_n^{(k)})}{d\theta}. \tag{B3}$$

b. Mean-square logarithmic error

The MSD estimation theory developed in the preceding sections is defined with respect to a Euclidean parameter space Λ . In the case of equilibrium probe thermometry, the space of temperatures is not a Euclidean parameter space. However, in the specific case of equilibrium probe thermometry of a thermalizing channel, the space of temperatures can be mapped into a Euclidean space by taking the logarithm [35, 44]

$$\lambda(\theta) = \log(\theta). \tag{B4}$$

The EMSD then takes the form of an *expected mean-square logarithmic error* (EMSLE) studied in the main text.

c. Van Trees inequality in thermometry

For the sake of generality we will stick to an arbitrary parameterization $\lambda(\theta)$, i.e. a one-to-one map $\lambda : \Theta \rightarrow \Lambda$, which is assumed to be differentiable. The Fisher information transforms under a change of parameterization as

$$h_k(\lambda) = (d\theta/d\lambda)^2 h_k(\theta). \tag{B5}$$

Here, the data is obtained via projective energy measurements of the probe system. In fact, this is the optimal measurement maximising the Fisher information, which thus constitutes then the so-called *quantum Fisher information* being directly related to the heat capacity of the probe, i.e. [15]:

$$C(\theta; H_n^{(k)}) = \theta^2 h_k(\theta), \quad (\text{B6})$$

which is a functional of the probe Hamiltonian. In terms of the probe heat capacity the posterior averaged Fisher information introduced in the preceding section takes the form

$$\text{EMSD}^{-1} \leq Q[p(\theta)] + \sum_{k=1}^m \int d\mathbf{x}_{k-1} p(\mathbf{x}_{k-1}) \int d\theta p(\theta|\mathbf{x}_{k-1}) \left[\frac{1}{\theta} \frac{d\theta}{d\lambda} \right]^2 C(\theta; H_n^{(k)}). \quad (\text{B7})$$

where we have made use of the parameterization invariance of the probability density, i.e. $d\lambda p(\lambda|\mathbf{x}) = d\theta p(\theta|\mathbf{x})$, which is a requirement on a well-defined probability density. For convenience, we define

$$J_\lambda(\theta) := \left[\frac{1}{\theta} \frac{d\theta}{d\lambda} \right], \quad (\text{B8})$$

and note that in the specific case of $\lambda(\theta) = \log(\theta)$ it follows that $J_\lambda(\theta) = 1$, in which case we recover the form of the Van Trees inequality given in the main text. Lastly, we note that when working with the logarithmic parameterization, the Bayesian information of the prior takes the form

$$Q[p(\theta)] = \int d\theta p(\theta) [1 + \partial_\theta \log p(\theta)]^2 \quad (\text{B9})$$

We are interested in the optimal probe design, and formally define the optimization problem

$$\Gamma(\mathbf{x}_{k-1}) := \max_{H_n^{(k)}} \int d\theta p(\theta|\mathbf{x}_{k-1}) J_\lambda(\theta)^2 C(\theta; H_n^{(k)}) \quad (\text{B10})$$

Note that Γ is in general a functional of the past measurement trajectory, i.e., the optimal probe structure depends on the prior knowledge of the parameter to be estimated. In the following sections we derive model-independent upper bounds on Γ .

d. Model-independent super-extensive upper bound on Γ

In this section we derive a super-extensive bound on $\Gamma(\mathbf{x})$. Starting with Eq. (B10), we note that since the integrand is positive we can provide an upper bound by moving from a global maximization to a local maximization, i.e.

$$\Gamma(\mathbf{x}) \leq \int d\theta p(\theta|\mathbf{x}) J_\lambda^2(\theta) \max_H C(\theta; H). \quad (\text{B11})$$

The problem of maximizing the heat capacity, over all possible probe Hamiltonians at a given temperature, has been solved by Correa et al. [15]. The solution can be formulated as the temperature-independent tight upper bound

$$C(\theta; H) \leq \left[\frac{\xi_D}{2} \right]^2 - 1, \quad (\text{B12})$$

where ξ_D is the solution to the transcendental equation

$$e^{\xi_D} = (D-1) \frac{\xi_D + 2}{\xi_D - 2}. \quad (\text{B13})$$

This equation does not have a closed form solution. However, a general feature of the solution is that $\xi_D > \log(D-1)$, and that ξ_D approach $\log(D-1)$ from above as D becomes large. From this it follows that $\Gamma(\mathbf{x})$ satisfies the super-extensive upper bound

$$\Gamma(\mathbf{x}) \leq (\xi_D/2 - 1) (\xi_D/2 + 1) \int d\theta p(\theta|\mathbf{x}) J_\lambda^2(\theta), \quad (\text{B14})$$

which grows super-extensively in $\log(D)$. If we average $\Gamma(\mathbf{x})$ over the past measurement trajectory we find

$$\int d\mathbf{x} p(\mathbf{x}) \Gamma(\mathbf{x}) \leq (\xi_D/2 - 1) (\xi_D/2 + 1) \langle J_\lambda^2 \rangle_{\text{prior}} \equiv C_D \langle J_\lambda^2 \rangle_{\text{prior}}, \quad (\text{B15})$$

where we have defined

$$\langle J_\lambda^2 \rangle_{\text{prior}} = \int d\theta p(\theta) J_\lambda^2(\theta). \quad (\text{B16})$$

This bound is expected to be approximately tight in the limit where the prior is local with respect to the width of the heat capacity. As we will see in the next section, designing a probe with a critical heat capacity at a certain temperature, i.e. one attaining the maximal heat capacity, will result in the width of the heat capacity decreasing as $1/\log(D)$. We thus see that saturating the super-extensive bound requires a prior probability distribution confined to a domain $\theta \in [\theta_c - \Delta/2, \theta_c + \Delta/2]$ where θ_c is the critical temperature and $\Delta = 1/\log(D)$. As D increase this corresponds to an increasing amount of prior information.

e. Tight upper bound on the thermal energy density

In this section we want to derive an upper bound on the thermal energy at a given temperature for any probe structure, subject to the dimensionality constraint $\dim H = D$ on the considered probes. We will find that the thermal energy density is upper bounded by the temperature. Define the maximum thermal energy for any probe structure as

$$E_{\max}(\theta) := \max_H E(\theta; H), \quad (\text{B17})$$

$$E(\theta; H) := \text{Tr}[H\omega(\theta; H)], \quad (\text{B18})$$

where $\omega(\theta; H)$ is a thermal state at temperature θ . We denote the energy eigenvalues of the probe Hamiltonian by $\{\varepsilon_l\}$, and for convenience set the ground-state energy to zero. If we take the derivative of the thermal energy, and equate to zero we obtain the condition

$$\varepsilon_l = \theta + E(\theta; H) =: \varepsilon, \quad (\text{B19})$$

which implies a $D - 1$ degeneracy in the first excited state. Evaluating the above condition for this probe structure leads to a transcendental equation for ε/θ which can be solved. The result is the temperature-dependent upper bound

$$E(\theta; H) \leq \theta \mathcal{W}_D \quad (\text{B20})$$

$$\mathcal{W}_D := W\left(\frac{D-1}{e}\right), \quad (\text{B21})$$

where W denotes the product logarithm, also called the *Lambert W* function. In the limit of large D the behaviour of the product logarithm is such that \mathcal{W}_D tends asymptotically to $\log(D)$ from below. We stress that the above bound on the thermal energy can be saturated by an effective two level probe with a $D - 1$ degenerate excited state, and a temperature-dependent energy gap.

f. Extensive bound for the non-adaptive scenario

We start with the second term in Eq (4) of the main text. Since the Hamiltonian remains constant throughout the protocol, i.e., $H_n^{(k)} = H_n \forall k$, this term can be rewritten as

$$\begin{aligned} \bar{\Gamma} &:= \sum_{k=1}^m \iint d\theta d\mathbf{x}_{k-1} p(\theta) p(\mathbf{x}_{k-1}|\theta) C(\theta; H_n) \\ &= m \int d\theta p(\theta) C(\theta; H_n). \end{aligned} \quad (\text{B22})$$

Integrating by parts—recall that $C(\theta; H_n) = \partial_\theta E(\theta; H_n)$ —and maximising over H_n gives

$$\bar{\Gamma} \leq m \max_{H_n} \int d\theta [-\partial_\theta p(\theta)] E(\theta; H_n), \quad (\text{B23})$$

where we assumed that $p(\theta)E(\theta; H_n)$ is smooth and vanishes at the boundaries. By defining \mathcal{R} as the temperature domain where $\partial_\theta p(\theta) \leq 0$ we have

$$\begin{aligned} \bar{\Gamma} &\leq m \max_{H_n} \int_{\mathcal{R}} d\theta [-\partial_\theta p(\theta)] E(\theta; H_n) \\ &\leq m \int_{\mathcal{R}} d\theta [-\partial_\theta p(\theta)] \max_{H_n} E(\theta; H_n) \end{aligned} \quad (\text{B24})$$

To make further progress, we use the upper bound on the energy of an n -body system at thermal equilibrium (with total dimension $D = d^n$) that is given by Eq. (B20):

$$\max_{H_n} E(\theta; H_n) \leq \theta \mathcal{W}_D \leq \theta n \log d \quad (\text{B25})$$

where the second equality is saturated as $n \gg 1$. Plugging these results back into Eq. (4) of the main text we obtain a no-go theorem for non-adaptive strategies [Result (ii)]

$$\text{EMSLE}^{-1} \stackrel{\text{non-adaptive}}{\leq} Q[p(\theta)] + f[p(\theta)] mn \log d, \quad (\text{B26})$$

where $f[p(\theta)] = \int_{\mathcal{R}} d\theta [-\partial_\theta p(\theta)]\theta$ is a functional of the prior. Crucially, the bound (B26) implies that, even with arbitrary control over the n -body Hamiltonian, one cannot go above a linear scaling in n with non-adaptive strategies (compare with the general bound given by Eq. (7) of the main text).

Our alternative bound follows the exact same procedure, except we first recall that the thermal energy can be expressed as $\theta^2 \partial_\theta \Psi(\theta; H)$, where the Massieu potential reads $\Psi(\theta; H) := \log \mathcal{Z}(\theta; H)$ with $\mathcal{Z}(\theta; H)$ being the partition function of the probe. Starting from Eq. (B22) and by performing twice integration by parts we get

$$\begin{aligned} \bar{\Gamma} &= m \int d\theta p(\theta) C(\theta; H_n) = -m \int d\theta [\partial_\theta p(\theta)] E(\theta; H) \\ &= m \int d\theta [\partial_\theta (\theta^2 \partial_\theta p(\theta))] \Psi(\theta; H), \end{aligned} \quad (\text{B27})$$

where again we take the vanishing and differentiability of the boundary terms in both integrations—that is $p(\theta)E(\theta; H_n)$ and $\theta^2 \partial_\theta p(\theta) \Psi(\theta; H)$ —as a restriction on the choice of parameterization. We can derive an upper bound on the optimal solution by noting that $\Psi(\theta; H) \geq 0$ —recall that the ground state energy is set to zero—and by introducing $\bar{\mathcal{R}} = \{\theta \mid \partial_\theta (\theta^2 \partial_\theta p(\theta)) \geq 0\}$. Then

$$\bar{\Gamma} \leq m \max_H \int_{\bar{\mathcal{R}}} d\theta [\partial_\theta (\theta^2 \partial_\theta p(\theta))] \Psi(\theta; H). \quad (\text{B28})$$

As the integrand is now positive we can maximize the Massieu potential locally. Since the logarithm is monotonically increasing in its argument, this corresponds to substituting the largest value of the partition function, i.e. the Hilbert space dimension. The bound then takes the form

$$\begin{aligned} \bar{\Gamma} &\leq m \log(D) \int_{\bar{\mathcal{R}}} d\theta [\partial_\theta (\theta^2 \partial_\theta p(\theta))] \\ &\leq m \log(D) \{\theta^2 \partial_\theta p(\theta)\}_{\bar{\mathcal{R}}} \\ &=: m \log(D) g[p(\theta)], \end{aligned} \quad (\text{B29})$$

where $g[p(\theta)]$ is a functional of the prior distribution but independent of the probe. This gives two complementary bounds on $\bar{\Gamma}$, i.e. one expressed in terms of $f[p(\theta)]$ as presented in the main text, and one in terms of $g[p(\theta)]$. Which of these two is tighter depends on the specific prior.

Appendix C: The EMSLE for small number of interacting qubits: adaptive vs non-adaptive

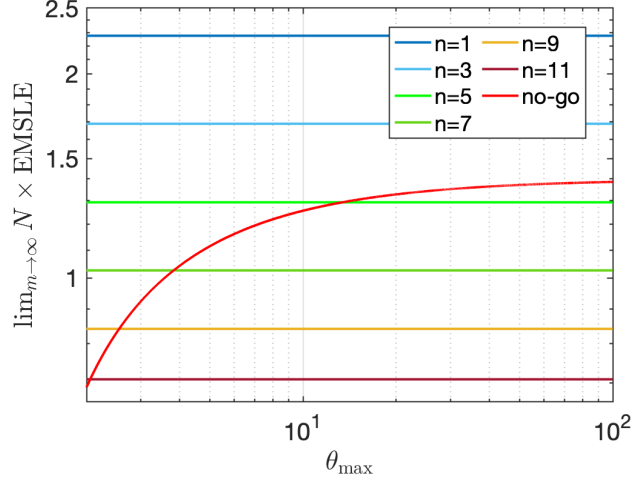


FIG. 4. The asymptotic value of normalised error, $\lim_{m \rightarrow \infty} N \times \text{EMSLE}$ (here $m = 2 \times 10^5$) vs the maximum temperature in the prior θ_{\max} , for the non-adaptive no-go theorem given by Eq. (12) of the main text (red curve). The horizontal lines show the same quantity in the adaptive scenario when using interacting qubits. One can see that for $\theta_{\max} \geq 20$ and by setting $n \geq 5$ the adaptive strategy overperforms any non-adaptive strategy. Here we set $\theta_{\min} = 1$ and $\alpha = -20$.

In the main text we demonstrated that by choosing $n > 10$ the adaptive strategy can reach a precision that any non-adaptive counterpart cannot reach (Fig. 2 of the main text, right panel). The exact value of interacting qubits n for which the adaptive strategy beats the non-adaptive no-go bound depends on the prior. For instance, in Fig. 4 we see that for some priors, adaptive strategies with $n = 5$ can beat the no-go theorem. We also emphasize that the no-go bound is not necessarily tight, in practice non-adaptive strategies might be far from them.

Nonetheless, one might still wonder about the experimental preparation of effectively two level probes with maximally degenerate excited state. In an upcoming paper, some of us show that similar energy structures can be prepared with spin Hamiltonians that contain only two-body interactions [60]. Yet still, our adaptive scheme is advantageous even in a single qubit or two qubits scenario (i.e., $n \in \{1, 2\}$), with two effective energy levels and a tunable gap.

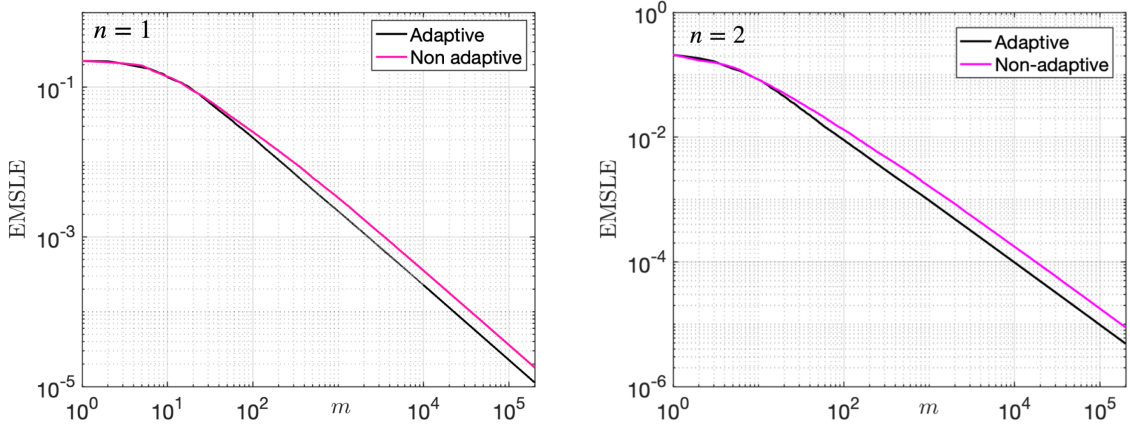


FIG. 5. The illustration of superiority of adaptive strategies vs non-adaptive ones. Clearly for sufficiently large repetitions the adaptive scheme overperforms the non-adaptive one. In particular, to reach the same target error $\text{EMSLE} = \mathcal{O}(2 \times 10^{-5})$ one needs about 60% less repetitions in the adaptive scenario compared to the non-adaptive scheme for $n = 1$ as depicted on the left panel (similarly, one needs about 80% less measurements for $n = 2$, as depicted on the right panel). Here the prior is the same as Eq. (13) of the main text with $\theta_{\min} = 1$, $\theta_{\max} = 10$, and $\alpha = -20$.

As illustrated in Fig. 5 one sees that to reach the same target error ($\text{EMSLE} = \mathcal{O}(2 \times 10^{-5})$), the adaptive scheme

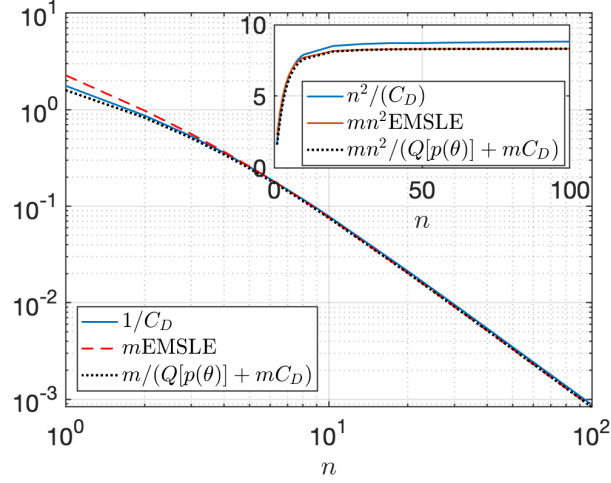


FIG. 6. The non-asymptotic behaviour of the EMSLE (here $m = 100$). Inspecting the inset above, one can see that, unlike the high m regime here we have $m\text{EMSLE} \neq 1/C_D$. This is so because the term $Q[p(\theta)]$ still plays a prominent role. In fact, if we incorporate this term, the inequality (7) of the main text will reduce to equality even for such a small number of repetitions.

requires roughly 60% less measurement runs compared to the non-adaptive strategy for $n = 1$, while for $n = 2$ the adaptive strategy requires roughly 80% less measurement runs.

Appendix D: The non-asymptotic EMSLE

In the main text we demonstrated how our proposed adaptive scheme can saturate the ultimate bound Eq. (7) of the main text, as depicted in Fig. 3 of the main text. The saturability of the bound is guaranteed by choosing high enough number of repetitions ($m = 2000$ in the main text). In case we were to perform less measurements, the bound is not generally saturated. Moreover, the first term in the r.h.s. of Eq. (7), i.e., $Q[p(\theta)]$ will also play a role. This is depicted in Fig. 6.